

# A New Organic–Inorganic Hybrid Layered Molybdenum(V) Cobalt Phosphate Constructed from $[\text{H}_{24}(\text{Mo}_{16}\text{O}_{32})\text{Co}_{16}(\text{PO}_4)_{24}(\text{OH})_4(\text{C}_5\text{H}_4\text{N})_2(\text{H}_2\text{O})_6]^{4-}$ Wheels and 4,4'-Bipyridine Linkers

Kai Yu,<sup>†</sup> Bai-Bin Zhou,<sup>\*,†</sup> Yang Yu,<sup>†</sup> Zhan-Hua Su,<sup>†</sup> and Guo-Yu Yang<sup>\*,‡</sup>

<sup>†</sup>Key Laboratory of Synthesis of Functional Materials and Green Catalysis, Colleges of Heilongjiang Province, Harbin Normal University, Harbin 150025, People's Republic of China, and <sup>‡</sup>State Key Laboratory of Structural Chemistry, Fujian Institute of Research on the Structure of Matter, Fuzhou, Fujian 350002, People's Republic of China

Received November 11, 2010

A new layered molybdenum cobalt phosphate,  $\text{Na}_2[\text{Co}(\text{H}_2\text{O})_6][(\text{Mo}_{16}\text{O}_{32})\text{Co}_{16}(\text{PO}_4)_{24}(\text{HPO}_4)_{16}(\text{H}_2\text{PO}_4)_4(\text{OH})_4(\text{C}_{10}\text{H}_8\text{N}_2)_4(\text{C}_5\text{H}_4\text{N})_2(\text{H}_2\text{O})_6] \cdot 4\text{H}_2\text{O}$  (**1**), has been hydrothermally synthesized and structurally characterized. **1** crystallizes in the monoclinic space group  $P2_1/n$  with  $a = 15.6825(18)$  Å,  $b = 39.503(4)$  Å,  $c = 17.2763(17)$  Å,  $\beta = 93.791(2)^\circ$ ,  $V = 10679.4(18)$  Å<sup>3</sup>, and  $Z = 2$ . A polyoxoanion of **1** exhibits an unusual organic–inorganic hybrid wheel-type cluster, in which two pyridine ligands link to the surface  $\text{Co}^{\text{II}}$  atoms of a  $[\text{H}_{24}(\text{Mo}_{16}\text{O}_{32})\text{Co}_{16}(\text{PO}_4)_{24}(\text{OH})_4(\text{H}_2\text{O})_6]$  (namely,  $\{\text{Mo}_{16}\text{Co}_{16}\text{P}_{24}\}$ ) wheel via the Co–N bonds. Furthermore, each  $\{\text{Mo}_{16}\text{Co}_{16}\text{P}_{24}\}$  wheel is connected to four adjacent wheels by four pairs of 4,4'-bipyridine linkers, forming a 2D layered network. The susceptibility measurement shows the existence of dominant antiferromagnetic interactions in **1**.

## Introduction

Polyoxometalate (POM)-based organic–inorganic hybrid compounds have attracted great interest in recent years owing to not only their variety of architectures and topologies but also their numerous potential applications in catalysis, medicine, and fluorescent, electronic, and magnetic materials.<sup>1</sup> A current research interest in this field is modification

to the surface of POMs with various organic and/or transition-metal complex moieties.<sup>1–10</sup> These kinds of modified POM derivatives can be regarded as ideal molecular materials because they combine the properties of the POM and those of the metal or the organic ligands. So, the compounds can be molecularly fine-tuned and provide potentially new types of

\*To whom correspondence should be addressed. E-mail: zhou\_bai\_bin@sina.com (B.-B.Z.), ygy@fjirsm.ac.cn (G.-Y.Y.). Tel: (+86) 0451-88060770. Fax: (+86) 591-8371-0051.

(1) (a) Gouzerh, P.; Proust, A. *Chem. Rev.* **1998**, *98*, 77. (b) Gouzerh, P.; Villanneau, R.; Delmont, R.; Proust, A. *Chem.—Eur. J.* **2000**, *6*, 1184. (c) Pope, M. T.; Müller, A. *Angew. Chem., Int. Ed. Engl.* **1991**, *30*, 34. (d) Long, D. L.; Burkholder, E.; Cronin, L. *Chem. Soc. Rev.* **2007**, *36*, 105.

(2) (a) Hagrman, P. J.; Hagrman, D.; Zubieta, J. *Angew. Chem., Int. Ed.* **1999**, *38*, 2638. (b) Burkholder, E.; Golub, V.; O'Connor, C. J.; Zubieta, J. *Inorg. Chem.* **2003**, *42*, 6729. (c) Burkholder, E.; Golub, V.; O'Connor, C. J.; Zubieta, J. *Inorg. Chem.* **2004**, *43*, 7014. (d) Bassil, B. S.; Dickman, M. H.; Römer, I.; von der Kammer, B.; Kortz, U. *Angew. Chem., Int. Ed.* **2007**, *46*, 6192.

(3) (a) Fang, X. K.; Anderson, T. M. C.; Benelli, Hill, C. L. *Chem.—Eur. J.* **2005**, *11*, 712. (b) Pradeep, C. P.; Long, D. L.; Kögerler, P.; Cronin, L. *Chem. Commun.* **2007**, 4254. (c) Zheng, S. T.; Yuan, D. Q.; Jia, H. P.; Zhang, J.; Yang, G. Y. *Chem. Commun.* **2007**, 1858. (d) Pichon, C.; Mialane, P.; Dolbecq, A.; Marrot, J.; Rivière, E.; Keita, B.; Nadjo, L.; Sécheresse, F. *Inorg. Chem.* **2007**, *46*, 5292.

(4) (a) Bareyt, S.; Piligkos, S.; Hasenknopf, B.; Gouzerh, P.; Lacôte, E.; Thorimbert, S.; Malacria, M. *Angew. Chem., Int. Ed.* **2003**, *42*, 3404. (b) Johns, B. J. S.; Schroden, R. C.; Zhu, C. C.; Stein, A. *Inorg. Chem.* **2001**, *40*, 801. (c) Hayashi, K.; Murakami, H.; Nomiyama, K. *Inorg. Chem.* **2006**, *45*, 8078. (d) Sakai, Y.; Shinohara, A.; Hayashi, K.; Nomiyama, K. *Eur. J. Inorg. Chem.* **2006**, 163.

(5) (a) Reinoso, S.; Vitoria, P.; Felices, L. S.; Lezama, L.; Gutiérrez - Zorrilla, J. M. *Inorg. Chem.* **2006**, *45*, 108. (b) Bar-Nahum, I.; Etedgui, J.; Konstantinovski, L.; Kogan, V.; Neumann, R. *Inorg. Chem.* **2007**, *46*, 5798. (c) Bar-Nahum, I.; Cohen, H.; Neumann, R. *Inorg. Chem.* **2003**, *42*, 3677.

(6) (a) Zheng, S. T.; Zhang, J.; Yang, G. Y. *Angew. Chem., Int. Ed.* **2008**, *47*, 3909. (b) Fang, X. K.; Anderson, T. M.; Hill, C. L. *Angew. Chem., Int. Ed.* **2005**, *44*, 3540. (c) Zhao, J. W.; Zhang, J.; Zheng, S. T.; Yang, G. Y. *Chem. Commun.* **2008**, 570. (d) Fang, X. K.; Anderson, T. M.; Hou, Y.; Hill, C. L. *Chem. Commun.* **2005**, 5044.

(7) (a) Zhao, J. W.; Wang, C. M.; Zhang, J.; Zheng, S. T.; Yang, G. Y. *Chem.—Eur. J.* **2008**, *14*, 9223. (b) Yoshida, A.; Yoshimura, M.; Uehara, K.; Hikichi, S.; Mizuno, N. *Angew. Chem., Int. Ed.* **2006**, *45*, 1956. (c) Laronze, N.; Marrot, J.; Hervé, G. *Chem. Commun.* **2003**, 2360.

(8) (a) Zhang, Q. H.; Cao, C. J.; Xu, T.; Su, M.; Zhang, J. Z.; Wang, Y. *Chem. Commun.* **2009**, 2376. (b) Shi, S. Y.; Sun, Y. H.; Chen, Y.; Xu, J. N.; Cui, X. B.; Wang, Y.; Wang, G. W.; Yang, G. D.; Xu, J. Q. *Dalton Trans.* **2010**, 39, 1389. (c) Jin, H.; Qi, Y. F.; Wang, E. B.; Li, Y. G.; Wang, X. L.; Qin, C.; Chang, S. *Cryst. Growth Des.* **2006**, *6*, 2693.

(9) (a) Liu, C. G.; Guan, W.; Song, P.; Su, Z. M.; Yao, C.; Wang, E. B. *Inorg. Chem.* **2009**, *48*, 8115. (b) Lou, D.; Tan, H. Q.; Chen, W. L.; Li, Y. G.; Wang, E. B. *CrystEngComm* **2010**, *12*, 2044.

(10) (a) Chang, W. J.; Jing, Y. C.; Wang, S. L.; Lii, K. H. *Inorg. Chem.* **2006**, *45*, 6586. (b) Wang, J. P.; Zhao, J. W.; Ma, P. T.; Ma, J. C. L.; Yang, P.; Bai, Y.; Li, M. X.; Niu, J. Y. *Chem. Commun.* **2009**, 2362. (c) Zhang, X.; Yi, Z.; Zhao, L. Y.; Chen, Q.; Wang, X. L.; Xu, J. Q.; Xia, W. J.; Yang, C. *CrystEngComm* **2010**, *12*, 595.

catalyst systems as well as interesting functional materials with optical, electronic, and magnetic properties.<sup>1</sup> During the preparation, two strategies have been exploited to increase the surface charge density and activate the surface O atoms of heteropolyoxoanions: (1) reduce the metal centers from high oxidation state to low oxidation state, for example, from Mo<sup>VI</sup> to Mo<sup>V</sup>, by introducing strong reducing reagents; (2) replace high-valence metal centers with lower-valence ones, for instance, from Mo<sup>VI</sup> to V<sup>IV</sup> or TM<sup>2+</sup> (TM = transition metal). However, the highly reduced polyoxoanions are usually unstable and inclined to be oxidized in an ambient atmosphere. Thus, the hydrothermal technique has been extensively employed and proved to be an efficient way to obtain the metastable POMs modified by various organic and/or metal–organic fragments.<sup>2</sup> In the POM field, the reduced molybdenum phosphates receive much attention for their applications in catalysis, ion exchange, and molecular sieves. On the basis of the above strategies, a series of new reduced polymolybdophosphates decorated with organic units were made.<sup>2b,c,9–12</sup> More recently, three unusual large clusters, [H<sub>14</sub>(Mo<sub>16</sub>O<sub>32</sub>)Co<sub>16</sub>(PO<sub>4</sub>)<sub>24</sub>(H<sub>2</sub>O)<sub>20</sub>]<sup>9–</sup>,<sup>13a</sup> [H<sub>18</sub>–(Mo<sub>16</sub>O<sub>32</sub>)Ni<sub>16</sub>(PO<sub>4</sub>)<sub>26</sub>(OH)<sub>6</sub>(H<sub>2</sub>O)<sub>8</sub>]<sup>18–</sup>,<sup>13b</sup> and [H<sub>30</sub>(Mo<sub>16</sub>O<sub>32</sub>)Ni<sub>14</sub>(PO<sub>4</sub>)<sub>26</sub>O<sub>2</sub>(OH)<sub>4</sub>(H<sub>2</sub>O)<sub>8</sub>]<sup>13c</sup> have been reported. However, no organic or metal–organic complexes have been successfully introduced to these highly reduced polymolybdophosphate clusters so far. This is because the large size of the POMs decreases the electron density of the surface or the coordination ability of the surface O atoms. As our continuing research work on organic–inorganic hybrid {MoO<sub>x</sub>/P/TM/L} systems, we are interested in using organic ligands to decorate high-nuclear polymolybdophosphate clusters. Here, a new 2D layered organic–inorganic hybrid molybdenum cobalt phosphate, Na<sub>2</sub>[Co(H<sub>2</sub>O)<sub>6</sub>][(Mo<sub>16</sub>O<sub>32</sub>)Co<sub>16</sub>(PO<sub>4</sub>)<sub>4</sub>(HPO<sub>4</sub>)<sub>16</sub>(H<sub>2</sub>PO<sub>4</sub>)<sub>4</sub>(OH)<sub>4</sub>(C<sub>10</sub>H<sub>8</sub>N<sub>2</sub>)<sub>4</sub>(C<sub>5</sub>H<sub>4</sub>N)<sub>2</sub>(H<sub>2</sub>O)<sub>6</sub>]·4H<sub>2</sub>O (**1**), has been successfully made under hydrothermal conditions, in which the organic ligands, pyridine (py) and 4,4′-bipyridine (4,4′-bipy), are not only introduced into the {Mo/TM/P} system, forming the wheel-type cluster [H<sub>24</sub>–(Mo<sub>16</sub>O<sub>32</sub>)Co<sub>16</sub>(PO<sub>4</sub>)<sub>24</sub>(OH)<sub>4</sub>(H<sub>2</sub>O)<sub>6</sub>] (namely, {Mo<sub>16</sub>Co<sub>16</sub>P<sub>24</sub>}), but also link the {Mo<sub>16</sub>Co<sub>16</sub>P<sub>24</sub>} wheels by 4,4′-bipy linkers to form the first organic–inorganic hybrid polymolybdophosphates.

## Experimental Section

**General Methods and Materials.** All chemicals were commercially purchased and used without further purification. Elemental analyses (C, H, and N) were performed on a Perkin-Elmer 2400 CHN elemental analyzer. Na, P, Mo, and Co analyses were performed on a PLASMA-SPEC (I) inductively coupled plasma atomic emission spectrometer. The IR spectrum was recorded in the range 400–4000 cm<sup>−1</sup> on an Alpha Centaur FT/IR spectrophotometer using KBr pellets. X-ray photoelectron spectroscopy (XPS) analyses were performed on a VG ESCALAB MK II spectrometer with a Mg Kα (1253.6 eV) achromatic X-ray source. The vacuum inside the analysis chamber was maintained at 6.2 × 10<sup>−6</sup> Pa during analysis. Thermogravimetric (TG) analyses were performed on a Perkin-Elmer TGA7 instrument in flowing O<sub>2</sub> with a heating rate of 10 °C·min<sup>−1</sup>. Magnetic

**Table 1.** Crystal Data and Structure Refinements for Complex **1**

empirical formula	C <sub>50</sub> H <sub>100</sub> N <sub>10</sub> Na <sub>2</sub> Co <sub>17</sub> Mo <sub>16</sub> P <sub>24</sub> O <sub>148</sub>
fw, g	6535.52
temperature, K	273(2)
cryst syst	monoclinic
space group	P2 <sub>1</sub> /n
a, Å	15.6825(15)
b, Å	39.503(4)
c, Å	17.2763(17)
α, deg	90
β, deg	93.791(2)
γ, deg	90
V, Å <sup>3</sup>	10679.4(18)
Z	2
D <sub>calc</sub> , Mg·m <sup>−3</sup>	2.031
μ, mm <sup>−1</sup>	2.470
F(000)	6326.0
data/params	91 862/26 437
R <sub>int</sub>	0.1399
GOF	1.072
final R indices [I > 2σ(I)]	R1 = 0.0587, wR2 = 0.1435
R indices (all data) <sup>a</sup>	R1 = 0.0771, wR2 = 0.1618

$$^a R1 = \frac{\sum(|F_o| - |F_c|)/\sum|F_o|}{\sum|F_o|}; wR2 = \frac{\{\sum[w(|F_o|^2 - |F_c|^2)]^2\}}{\sum[w(|F_o|^2)]^{1/2}}$$

susceptibility measurements of compound **1** were performed using a Quantum Design SQUID magnetometer (MPMS-XL) with polycrystalline samples. Experimental data were corrected for the sample holder and for the sample's diamagnetic contribution calculated from Pascal constants.

**Syntheses of Na<sub>2</sub>[Co(H<sub>2</sub>O)<sub>6</sub>][(Mo<sub>16</sub>O<sub>32</sub>)Co<sub>16</sub>(PO<sub>4</sub>)<sub>4</sub>(HPO<sub>4</sub>)<sub>16</sub>(H<sub>2</sub>PO<sub>4</sub>)<sub>4</sub>(OH)<sub>4</sub>(C<sub>10</sub>H<sub>8</sub>N<sub>2</sub>)<sub>4</sub>(C<sub>5</sub>H<sub>4</sub>N)<sub>2</sub>(H<sub>2</sub>O)<sub>6</sub>]·4H<sub>2</sub>O (**1**).** A mixture of Na<sub>2</sub>MoO<sub>4</sub>·2H<sub>2</sub>O (1.452 g, 6.00 mmol), Co(CH<sub>3</sub>COO)<sub>2</sub>·4H<sub>2</sub>O (0.480 g, 2.52 mmol), 4,4′-bipyridine (0.400 g, 2.70 mmol), H<sub>3</sub>PO<sub>4</sub> (2 mL, 30 mmol), and pyridine (0.350 g, 4.42 mmol) was dissolved in 36 mL of water. The mixture was stirred for 0.5 h at room temperature and the pH adjusted to 2.5 with 1 M NaOH. The resulting suspension was sealed in a 50-mL Teflon-lined stainless steel autoclave and heated at 165 °C for 5 days. After cooling to room temperature, the deep-red block crystals were isolated. The crystals were filtered, washed with distilled water, and dried at room temperature with a yield of 45% (based on Co). Anal. Calcd for C<sub>50</sub>H<sub>100</sub>N<sub>10</sub>Na<sub>2</sub>O<sub>148</sub>P<sub>24</sub>Mo<sub>16</sub>Co<sub>17</sub> (M<sub>r</sub> = 6535.52): C, 9.19; H, 1.55; N, 2.14; Na, 0.70; P, 11.37; Mo, 23.49; Co, 15.33. Found: C, 9.22; H, 1.52; N, 2.16; Na, 0.68; P, 11.35; Mo, 23.51; Co, 15.37. IR (KBr pellets, cm<sup>−1</sup>): 3314(br), 3089(br), 1643(s), 1520(m), 1428(m), 1125(s), 983(s), 849(s), 747(s), 510(w)

**X-ray Crystallography.** A single crystal of **1** (dimensions of 0.27 × 0.25 × 0.23 mm) was mounted on a glass fiber, and data were collected on a Bruker SMART CCD diffractometer with graphite-monochromated Mo Kα radiation (λ = 0.710 73 Å). A semiempirical absorption correction based on symmetry-equivalent reflections was applied. A total of 26 853 reflections were collected, of which 12 865 reflections were unique (R<sub>int</sub> = 0.1399). The structure was solved by direct methods and refined by the full-matrix least-squares method based on F<sup>2</sup>. Structure solution, refinement, and generation of publication materials were performed with the use of the *SHELXTL* crystallographic software package.<sup>20</sup> All of the non-H atoms were refined with anisotropic parameters. The H atoms on the C atoms of py and 4,4′-bpy were included in calculated positions with the use of a riding model and refined with fixed isotropic thermal parameters. The H atoms on water molecules were not included and just put into the final molecular formula. A summary of the crystal data is presented in Table 1. The CCDC number is 800818 for **1**.

## Results and Discussion

**Synthesis.** **1** was only made by a hydrothermal technique. Under hydrothermal conditions, many factors may

(11) (a) Thomas, J.; Ramanan, A. *Cryst. Growth Des.* **2008**, *8*, 3390. (b) Jin, H. J.; Zhou, B. B.; Yu, Y.; Zhao, Z. F.; Su, Z. H. *Cryst. Eng. Comm.* **2010**, DOI: 10.1039/c004063k.

(12) (a) Yu, K.; Li, Y. G.; Zhou, B. B.; Su, Z. H.; Zhao, Z. F.; Zhang, Y. N. *Eur. J. Inorg. Chem.* **2007**, 5662. (b) Zhang, X. M.; Wu, H. S.; Zhang, F. Q.; Prikhod'ko, A.; Kuwata, S.; Comba, P. *Chem. Commun.* **2004**, 2046.

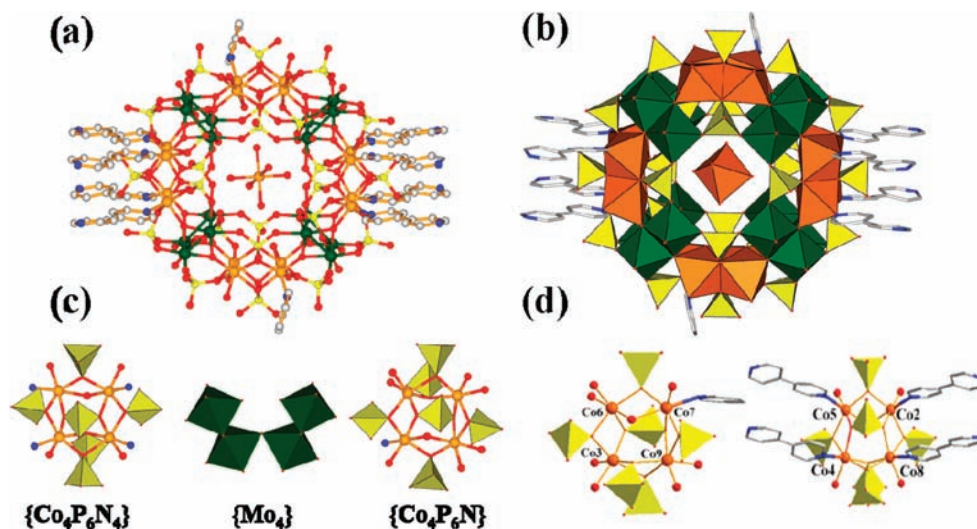


**Figure 1.** (a) Ball-and-stick representation of the hybrid wheel-type cluster of **1**. (b) Polyhedral representation of the hybrid wheel-type cluster of **1**. Color code: Mo, green; Co, orange; P, yellow; O, red; N, blue; C, gray. (c) Constituent units of the wheel-type cluster of **1**. (d) Coordination environment of cobalt in the hybrid wheel-type polyoxoanion of **1**.

effect the crystal growth and structure of the products, including the kind and stoichiometry of the starting materials, temperature, pH value, filling volume, and reaction time.<sup>2–14</sup> During our exploration on the new polyoxomolybdates in the {Mo/TM/P} system, a series of new organic–inorganic hybrids have been hydrothermally made. Most of these are based on the Keggin-type {PMo<sub>12</sub>} unit,<sup>8</sup> Dawson-class {P<sub>2</sub>Mo<sub>18</sub>} cluster,<sup>9</sup> {P<sub>4</sub>Mo<sub>6</sub>} fragment,<sup>10</sup> {P<sub>2</sub>Mo<sub>5</sub>} anion,<sup>11</sup> the basket-like {P<sub>6</sub>Mo<sub>18</sub>} cage,<sup>12</sup> and the {Mo<sub>16</sub>TM<sub>16</sub>P<sub>26</sub>} wheel.<sup>13</sup> We are interested in inorganic–organic hybrids based on the {Mo<sub>16</sub>TM<sub>16</sub>P<sub>26</sub>} wheel because these systems have not been systemically explored. Two important factors must be fully considered during the synthesis: (1) The proper reductive reagent must be introduced into the reaction system for reducing the Mo<sup>VI</sup> center to Mo<sup>V</sup>. (2) The formation conditions of the wheel must be satisfied, i.e., to enable TM and phosphate groups to connect to Mo fragments, forming large clusters. So, it is necessary to select suitable acidity and reaction temperature. In the initial stages of the reaction, although various molar ratios of Na<sub>2</sub>MoO<sub>4</sub>·H<sub>3</sub>PO<sub>4</sub>:TM<sup>2+</sup>:L have been applied, the initial pH values, reductive reagent, and reaction temperature seem to be vital to the reaction.<sup>13</sup> It is worth mentioning that the wheel-type {Mo<sub>16</sub>TM<sub>16</sub>P<sub>26</sub>} clusters were generally made above 160 °C within the pH range of 2.0–4.0. Furthermore, the use of the Mo metal, amino acid (DL- $\alpha$ -alanine), and chelate ligands with carboxyl groups (H<sub>4</sub>EDTA) as the reductive reagent is an effective method. In our case, the py and 4,4'-bpy ligands plays three roles in the formation of the hybrid wheel during the self-assembly process: (1) they can substitute the surface O atoms of the polyoxoanion; (2) they act as the reductive reagent to promote the reduction of Mo<sup>VI</sup> to Mo<sup>V</sup>; (3) they also serve in structure-directing roles. Through careful

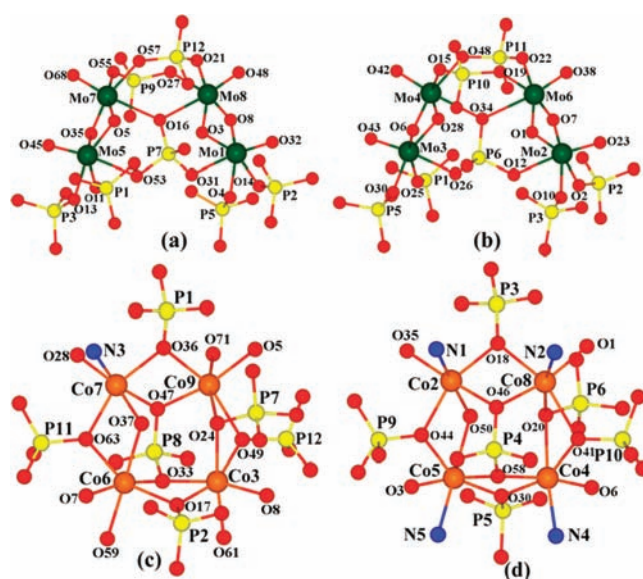


**Figure 2.** Ball-and-stick representation of four basic building blocks in the wheels of **1**: (a) first type of {Mo<sub>4</sub>} unit; (b) second type of {Mo<sub>4</sub>} unit; (c) first type of {Co<sub>4</sub>} unit; (d) second type of {Co<sub>4</sub>} unit.

exploration, the optimal reaction conditions for **1** is found to be a mixture of Na<sub>2</sub>MoO<sub>4</sub>·2H<sub>2</sub>O, Co(Ac)<sub>2</sub>·4H<sub>2</sub>O, H<sub>3</sub>PO<sub>4</sub>, py, and 4,4'-bpy in a molar ratio of 6:2.52:30:2.7:4.42 in water (pH 2.5) at 165 °C for 5 days. If the reaction temperature was lower than 165 °C or the pH value was outside of 2.5, no crystals were obtained.

**Structure of 1.** Single-crystal X-ray diffraction analysis revealed that compound **1** is a 2D layered structure constructed from the wheel-type cluster units [H<sub>24</sub>(Mo<sub>16</sub>O<sub>32</sub>)Co<sub>16</sub>(PO<sub>4</sub>)<sub>24</sub>(OH)<sub>4</sub>(H<sub>2</sub>O)<sub>6</sub>]<sup>4-</sup> modified with py ligands and 4,4'-bpy linkers, Co(H<sub>2</sub>O)<sub>6</sub> octahedra, sodium cations, and lattice H<sub>2</sub>O molecules (Figure S1 in the Supporting Information). The structural building unit can be described as a centrosymmetric wheel-shaped cluster with overall C<sub>2v</sub> symmetry (Figure 1a,b) containing four {Mo<sub>4</sub>} tetramers, two {Co<sub>4</sub>P<sub>6</sub>N<sub>4</sub>} fragments, and two {Co<sub>4</sub>P<sub>6</sub>N} units (Figure 1c), encapsulating a central

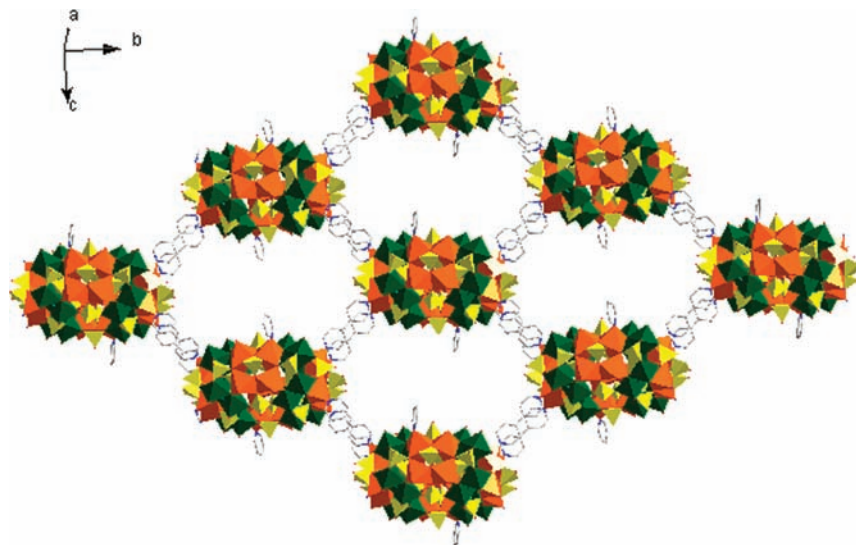
(13) (a) Peloux, C.; Dolbecq, A.; Mialane, P.; Marrot, J.; Rivière, E.; Sécheresse, F. *Angew. Chem., Int. Ed.* **2001**, *40*, 2455. (b) Peloux, C.; Dolbecq, A.; Mialane, P.; Marrot, J.; Rivière, E.; Sécheresse, F. *Inorg. Chem.* **2002**, *41*, 7100. (c) Zhang, Y. N.; Zhou, B. B.; Li, Y. G.; Su, Z. H.; Zhao, Z. F. *Dalton Trans.* **2009**, 9446.

(14) Boudreaux, E. A.; Mulay, L. N., Eds. *Theory and Applications of Molecular Paramagnetism*; John Wiley & Sons: New York, 1976.

**Table 2.** Coordination Environments of  $\{\text{PO}_4\}$  Groups in the Symmetric Unit of the Wheel in **1**

No.	$\text{PO}_4$ bridge	Number ( $\times 2$ )	Metal centers	P centers <sup>a</sup>	Protonated form	The coordination environments of $\{\text{PO}_4\}$ group
1	$\mu_4$ - $\text{PO}_4$	2	4 Co	P4, P8	$[\text{H}_2\text{PO}_4]^-$	
2	$\mu_4$ - $\text{PO}_4$	8	2 Mo (in the same tetramer), 2Co	P9-P12	$[\text{HPO}_4]^{2-}$	
			2 Mo (in the different tetramer), 2Co	P1-P3, P5	$[\text{HPO}_4]^{2-}$	
3	$\mu_6$ - $\text{PO}_4$	2	4 Mo, 2 Co	P6, P7	$[\text{PO}_4]^{3-}$	

<sup>a</sup> All P labels are consistent with those in Figure 2.

**Figure 3.** View of the 2D layered network in **1**.

$[\text{Co}(\text{H}_2\text{O})_6]^{2+}$  octahedron located on an inversion center. The outer size of the wheel is ca.  $16.8 \times 16.9 \text{ \AA}$ , while the inner cavity is ca.  $6.3 \times 6.4 \text{ \AA}$ .

In the structure, two types of  $\{\text{Mo}_4\}$  tetramers containing four  $\text{MoO}_6$  octahedra are reinforced by three phosphate groups (P7, P9, and P12 in Figure 2a and P6, P10, and P11 in Figure 2b) via a  $\mu_3$ -O atom (O16 and O34, respectively) and six  $\mu$ -O atoms (O48, O22, O15, O19, O26, O12 and O31, O53, O21, O57, O27, O55, respectively), in which each Mo atom adopts disordered octahedral geometry with Mo–Mo distances in the range of 2.600(3)–2.612(3)  $\text{\AA}$ .

Four  $\{\text{CoO}_6\}$  or  $\{\text{CoO}_{6-x}\text{N}_x\}$  ( $x = 1$  or 4) octahedra connect to each other in an edge-sharing mode and further are linked by six  $\text{PO}_4$  groups in a corner-sharing mode to form two types of  $\{\text{Co}_4\}$  tetramers (Figure 2c,d), resulting in the lower symmetry of the wheel, from  $C_{4v}$  in the reported wheel<sup>13a</sup> to  $C_{2v}$  in **1**. Furthermore, the number of coordinated water molecules within the wheel in **1** is different from all of the reported wheels<sup>13</sup> because of the varying coordination environments of some Co atoms. In one type of  $\{\text{Co}_4\}$  tetramer (Figure 2c), only one Co center of four Co octahedra linked to the N atom of the py ligand. The Co6 and Co7 centers are coordinated

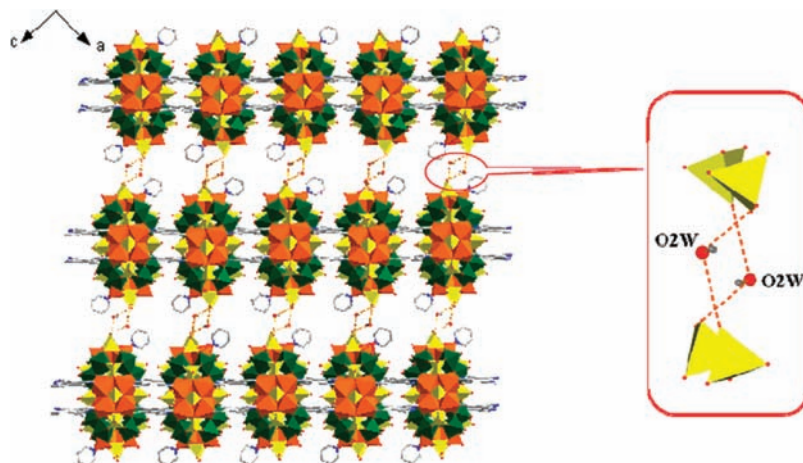


Figure 4. Polyhedral and ball-and-stick representation of the 3D framework along the *b* axis in **1**.

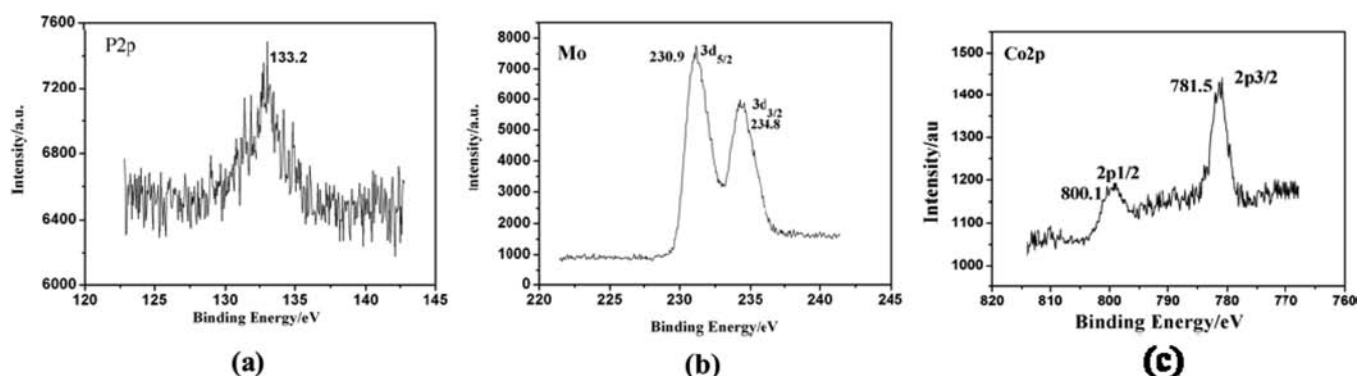


Figure 5. XPS spectra of compound **1**.

with three  $\mu_3$ -O atoms shared by two Co atoms and  $\text{PO}_4$  groups, one  $\mu_3$ -O atom shared by one Co and two Mo atoms, one  $\mu_2$ -OH (O37) atom shared by two Co atoms, and one terminal water ligand for the Co6 atom and one N atom of py for the Co7 atom, respectively. Both Co3 and Co9 centers are surrounded by four  $\mu_3$ -O atoms shared by two Co and  $\text{PO}_4$  groups, one  $\mu_3$ -O atom shared by one Co, two Mo atoms, and one water ligand (Figures 1d and 2c), respectively. The Co–O bond lengths are in the range of 2.032(14)–2.126(19) Å, and the Co–N bond length is 2.11(2) Å. In the other type of  $\{\text{Co}_4\}$  tetramer (Figure 2d), all octahedral Co centers link to the N atoms of the 4,4'-bpy ligands. The Co8 and Co4 centers coordinate to four  $\mu_3$ -O atoms shared by two Co and  $\text{PO}_4$  groups, one  $\mu_3$ -O atom shared by one Co and two Mo atoms, and one N atom of the 4,4'-bpy ligand, respectively. The Co5 and Co2 centers are surrounded by three  $\mu_3$ -O atoms shared by two Co and  $\text{PO}_4$  groups, one  $\mu_3$ -O atom shared by one Co and two Mo atoms, one  $\mu_2$ -OH (O50) atom shared by two Co atoms, and one N atom of the 4,4'-bpy ligand (Figures 1d and 2d), respectively. The bond lengths of Co–O are in the range of 2.011(14)–2.165(18) Å, and the bond lengths of Co–N are in the range of 2.125(19)–2.159(17) Å.

Bond valence sum (BVS) calculations<sup>15</sup> confirm that all Mo and Co centers are in the oxidation states of 5+ and 2+, respectively. In addition, BVS shows that the O atoms

located the protons of the phosphato groups (BVS values are in the range of 1.10–1.32), the hydroxo ligands (two O37 and two O50) only bridged two Co centers (0.69–0.84), and the terminal water ligands linked to the Co centers (0.29–0.34), respectively. Thus, the detailed formula of the hybrid wheel has been stated as  $[(\text{Mo}_{16}\text{O}_{32})(\text{PO}_4)_4(\text{HPO}_4)_4(\text{H}_2\text{PO}_4)_4\text{Co}_{16}(\text{OH})_4(\text{C}_5\text{H}_4\text{N})_2(\text{H}_2\text{O})_6]^{4-}$ .

The  $\{\text{Co}_4\}$  and  $\{\text{Mo}_4\}$  tetramers are alternately connected in a corner-sharing mode to form the cluster wheel. All  $\text{PO}_4$  groups as bridges or hinges are joined to the  $\{\text{Mo}_4\}$  or  $\{\text{Co}_4\}$  tetramers to reinforce the whole wheel-type structure except the  $\text{P}(4)\text{O}_4$  and  $\text{P}(8)\text{O}_4$  groups linked to four Co centers. According to the coordination environment of the  $\text{PO}_4$  groups in the wheel cluster, they can be separated into three types (Table 2), i.e., the  $\mu_4$ - $\text{PO}_4$  groups bridge four Co atoms, the  $\mu_2$ - $\text{PO}_4$  groups bridge two Mo and two Co atoms (Mo derived from the same  $\{\text{Mo}_4\}$  tetramers or adjacent  $\{\text{Mo}_4\}$  tetramers), and the  $\mu_6$ - $\text{PO}_4$  groups bridge four Mo and two Co atoms. Following the above-mentioned connection modes, there are 4  $\mu_4$ - $[\text{H}_2\text{PO}_4]^-$  bridges, 16  $\mu_2$ - $[\text{HPO}_4]^{2-}$  bridges, and 4  $\mu_6$ - $[\text{PO}_4]^{3-}$  bridges, respectively (Table 2).

Moreover, **1** exhibits a new linking mode that differs from the known 2D layered molybdenum(V) cobalt phosphate linked by cobalt dimers or monomers<sup>13a</sup> because each wheel in **1** connects the same four coplanar wheels by 4,4'-bpy linkers via four pairs of Co–N bonds, forming a 2D layer (Figure 3). Furthermore, these anionic layers are further linked together by lattice water

(15) Brown, D.; Altermatt, D. *Acta Crystallogr., Sect. B* **1985**, *41*, 244.

molecules (O2W) and the surface O atoms of polyoxoa-nions via hydrogen-bonding interactions to form a 3D supramolecular network (Figure 4).

**XPS.** The oxidation states of P, Mo, and Co are further confirmed by XPS spectra, which were carried out in the energy region of P 2p, Mo 3d<sub>5/2</sub>, Mo 3d<sub>3/2</sub>, Co 2p<sub>1/2</sub>, and Co 2p<sub>3/2</sub> (Figure 5). The peak at 133.2 eV is attributed to P<sup>5+</sup> ions, the peaks at 230.9 and 234.8 eV are ascribed to Mo<sup>5+</sup> ions,<sup>16</sup> and the peaks at 781.5 and 800.1 eV are ascribed to Co<sup>2+</sup> ions. Their oxidation states are in accordance with the valence bond calculations.

**IR Spectroscopy.** In the IR spectrum of compound **1** (Figure S2 in the Supporting Information), the peaks at 3314, 3089, and 1643 cm<sup>-1</sup> are ascribed to the vibrations of the lattice and coordinated water molecules. The characteristic peaks at 1520 and 1428 cm<sup>-1</sup> can be regarded as the vibrations of the py and 4,4'-bpy ligands. The strong bands at 1125, 983, and 747 cm<sup>-1</sup> are attributed to  $\nu(\text{P}-\text{O})$ ,  $\nu(\text{Mo}=\text{O})$ , and  $\nu(\text{Mo}-\text{O}-\text{Mo})$ , respectively. The peak located at 510 cm<sup>-1</sup> can be attributed to  $\nu(\text{Co}-\text{O})$ .

**TG Analysis.** In order to estimate the lattice–water content and the thermal stability of compound **1**, TG analysis was carried out from 25 to 800 °C. In the TG curve, there are three continuous weight loss steps (Figure S3 in the Supporting Information). The first weight loss of 4.36% in the temperature range of 60–250 °C corresponds to the release of all lattice and coordinated water molecules, which is in accordance with the calculated value of 4.41% (~16 H<sub>2</sub>O). The second weight losses of 16.30% in the temperature range of 250–580 °C are attributed to the loss of all py and 4,4'-bpy ligands and dehydration of the hydroxyls in **1**. The value is close to the calculated value of 15.83% (~2 py, 4 bpy, and 14 H<sub>2</sub>O). The last weight losses of 8.05% in the temperature range of 580–800 °C might be ascribed to the release of partial P<sub>2</sub>O<sub>5</sub> derived from mixed oxide phases.

**Magnetic Properties.** The variable-temperature magnetic susceptibility was measured from 300 to 2 K at 2000 Oe for **1** (Figure 6). The  $\chi_m T$  vs  $T$  curve shows a value of 47.79 emu·K·mol<sup>-1</sup> at 300 K, which continuously decreases upon cooling to a value of 7.39 emu·K·mol<sup>-1</sup> at 2 K, suggesting that antiferromagnetic interaction is predominant in **1**. Owing to spin pairing of the d<sup>1</sup> electrons in the Mo<sup>V</sup> dimers with the short Mo–Mo distances of an average value of 2.607 Å,<sup>17</sup> only the Co<sup>II</sup> ion is responsible for the magnetic properties of **1**. The effective magnetic moment per formula unit at 300 K, 19.55  $\mu_B$ , is in the range of experimentally observed values for 17 high-spin Co<sup>II</sup> ions with the orbital contribution.<sup>18</sup> Above 50 K, the magnetic susceptibility was fitted to a Curie–Weiss law, giving  $C = 52.4$  emu·K·mol<sup>-1</sup> and  $\theta = -27.5$  K. The large negative value of the Weiss constant should be related to both antiferromagnetic interactions and spin–orbit coupling effects. In **1**, besides the isolated Co(H<sub>2</sub>O)<sub>6</sub> cation, each wheel-type cluster unit contains four {Co<sub>4</sub>} tetramers connected with two {Mo<sub>4</sub>} tetramers in a corner-sharing mode. Considering the larger Co···Co distances (ca. 6.5 Å) between the {Co<sub>4</sub>} tetramers, magnetic

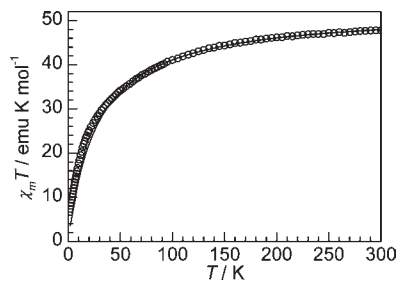


**Figure 6.** Plot of  $\chi_m T$  vs  $T$  for **1**. The solid line is the Curie–Weiss fit of the data.

exchange interactions should be mainly mediated by the double oxygen bridges between adjacent Co<sup>II</sup> ions within the {Co<sub>4</sub>} tetramers. The most important parameter considered in the magnetostructural correlation of the POM cores is the M–O–M angle. Structural analysis data reveal that the Co–O–Co bond angles range from 95.6° to 109.5°, with an average angle of 99.3°. Such values are in the range expected for antiferromagnetic coupling<sup>19</sup> and are consistent with our experimental observation.

## Conclusion

In conclusion, a novel molybdenum(V) cobalt phosphate containing an unusual organic–inorganic hybrid wheel-type cluster, Na<sub>2</sub>[Co(H<sub>2</sub>O)<sub>6</sub>][H<sub>24</sub>(Mo<sub>16</sub>O<sub>32</sub>)Co<sub>16</sub>(PO<sub>4</sub>)<sub>24</sub>(OH)<sub>4</sub>-(C<sub>10</sub>H<sub>8</sub>N<sub>2</sub>)<sub>4</sub>(C<sub>5</sub>H<sub>4</sub>N)<sub>2</sub>(H<sub>2</sub>O)<sub>6</sub>·4H<sub>2</sub>O (**1**), has been successfully made under hydrothermal conditions and structurally characterized. Interestingly, two different organic ligands modify the {Mo<sub>16</sub>TM<sub>16</sub>P<sub>26</sub>} wheel via the TM–N bonds, and each wheel connects to the same four wheels by four pairs of 4,4'-bpy to form a 2D layered network. Compound **1** represents a new member in the {Mo/TM/P} system and the first example of organic–inorganic hybrid wheel-type clusters. In order to investigate the effect of different reductive ligands on the POM products under hydrothermal conditions, further efforts will focus on the {Mo/TM/P/L} (L = organic ligands) system. Further work is in progress.

**Acknowledgment.** This work is supported by the National Natural Science Foundation of China (Grants 20671026 and 20971032), the Study Technological Innovation Project Special Foundation of Harbin (Grant 2009RFXXG202), the Science and Technology Project of Education Office of Heilongjiang Province (Project 11551122), the Technological innovation team building program of the college of Heilongjiang Province (Program 2009td04), and the Innovation Team Research Program of Harbin Normal University (Program KJTD200902).

**Supporting Information Available:** X-ray crystallographic files for compound **1** in CIF format and three plots (the molecular structural unit, the IR spectrum, and a TG curve; Figures S1–S3). This material is available free of charge via the Internet at <http://pubs.acs.org>.

(19) (a) Isele, K.; Gigon, F.; Williams, A. F.; Bernardinelli, G.; Franz, P.; Decurtins, S. *Dalton Trans.* **2007**, 332. (b) Xie, Y. S.; Liu, Q. L.; Jiang, H.; Ni, J. *Eur. J. Inorg. Chem.* **2003**, 4010.

(20) (a) Sheldrick, G. M. *SHELXL97, Program for Crystal Structure Refinement*; University of Göttingen: Göttingen, Germany, 1997. (b) Sheldrick, G. M. *SHELXS97, Program for Crystal Structure Solution*; University of Göttingen: Göttingen, Germany, 1997.

(16) Grim, S. O.; Matienzo, L. J. *Inorg. Chem.* **1975**, *14*, 1014.

(17) Vergamini, P. J.; Vahrenkamp, H.; Dahl, L. F. *J. Am. Chem. Soc.* **1971**, *93*, 6327.

(18) Carlin, R. L. *Magnetochemistry, Magnetochemistry*; Springer-Verlag: Berlin, 1986.